Screening of Zinc database to identify MurB enzyme inhibitors for *Staphylococcus aureus* pathogen

Luv Singhal [a], Apeksha Shrivastava [b], Neeraj Kumar [a], Chandra Shekhar Sharma [a*]

[a] *Department of Pharmaceutical Chemistry, Faculty of Pharmacy, Bhupal Nobles' University, Udaipur, Rajasthan 313001, India.*

[b] *Department of Pharmaceutical Chemistry, School of Pharmaceutical Education & Research, Jamia Hamdard, New Delhi-110062, India*

**Corresponding author email: cssmedchem@gmail.com*

Abstract: *Staphylococcus aureus* is a parasitic pathogen that is capable of causing lethal bacterial infections. The MurB (UDP-N-acetylenolpyruvylglucosamine reductase) enzyme is essential for the generation of peptidoglycan and the construction of the cell wall, which is an important component of a bacterial cell. *S. aureus* has become immune to most of the approved antibiotics, so it is essential to find new molecules for the treatment of ailments caused by this bacterium. In this research, ligands from the zinc database were subjected to pharmacokinetic evaluation using the QikProp module, and were filtered through the Lipinski filter. The resultant molecules were prepared using the LigPrep module, and the obtained compounds were screened through the 1HSK PDB ID of the MurB enzyme. The identified hits were subjected to molecular mechanics/generalized born and surface area studies to estimate the binding free energy of the docked complexes. Thereafter, the selected molecule, ZINC 34230491, was put through MD simulation studies of 100 ns each for determining the stability of the docked complex. The compound was found to be stable in the active site of the 1HSK PDB ID of the MurB protein, indicating that this compound could serve as a potential lead against the *S. aureus* pathogen.

Keywords: *Staphylococcus aureus,* MurB, structure-based virtual screening, pharmacokinetic evaluation, MD Simulations.

Introduction

Bacterial resistance has reduced the efficacy of antibiotics, and bacterial infections have increased in prevalence universally. *Staphylococcus aureus* is a member of the genus Staphylococcus, which is capable of causing a variety of severe infections [1]. In recent decades, due to the improper use of antibiotics, the drug resistance of *S. aureus* has steadily increased, the infection rate has risen globally, and the treatment has become more complicated [2]. *S. aureus* is the most prevalent pathogen responsible for septic infections, which can contribute to infections such as pneumonia, and pericarditis [3]. Infections caused by *S. aureus* bacteria account for more deaths than AIDS, tuberculosis, and viral hepatitis combined [4,5].

Disruption of cell wall assembly is a well-established and favored mechanism to develop antibiotics because of the lack of a eukaryotic homolog [11]. The β-lactam antibiotics, which bind to protein binding protein, and vancomycin, which binds to the Lipid II (cell wall precursor) are widely used antibiotics which function via this mechanism [11]. Bacterial cell wall is made of peptidoglycan which is a highly cross-linked polymer that is exclusive to microbial cells. The synthesis of cell wall require more than ten transformations, each carried out by an individual enzyme [12–14]. These enzymes are crucial for the survival of bacterial cells [11]. MurB enzyme is one such enzyme that catalyses the formation of UDP-Nacetylmuramic acid from UDP-N-acetylglucosamine [14], which plays crucial role in peptidoglycan biosynthesis [8–11]. Biochemical characterization and X-ray structural analysis of MurB from *Escherichia coli* [8,15,16], *Staphylococcus aureus* [8], and *Streptococcus pneumoniae* [17] have been published and utilized in structure-based drug design [18]. For the present study, we utilized 1HSK PDB ID of the MurB enzyme derived from *S. aureus* [8].

Virtual screening has emerged as an expeditious approach for identifying ligands that possess the ability to bind to a specific target. The methodology of structure-based virtual screening involves the comprehensive analysis of the active site's structure during the process of ligand discovery. This approach presents a superior alternative to ligand-based screening, which relies on a ligand-based hypothesis and matches the pharmacophoric feature, usually limited to 4-5 features [6,7]. From this standpoint, the compounds sourced from the Zinc database underwent virtual screening on the MurB enzyme (PDB ID: 1HSK) [8].

Materials & Methods

All the work (except MD simulation) was performed on Maestro *v*11.2 software installed on Lenovo 30B4A21900 workstation having Intel(R) Xeon(R) CPU E5-2620 v3 @ 2.40 GHz Processor, Windows 7 Operating System; 16 GB RAM; and 4 GB NVIDIA Quadro K620 graphics card. MD Simulation was performed by Desmond on Ubuntu 2022.04 system, Ryzen 9 5950X processor.

Protein Preparation:

The X-ray crystallographic structure of receptor MurB (PDB ID: 1HSK, co-crystallized ligand: FAD) [8], was downloaded from RCSB protein data bank. The enzyme belonged to *S. aureus* organism. The downloaded PDB ID was subjected to protein preparation wizard of Maestro. The protein was corrected for missing hydrogen atoms and for bond orders and it was then filled in with missing side chains and missing loops with the help of Prime *v*2.1 while pre-processing. All the water molecules except the water molecules of active site were removed [19]. All other ligands except the orthosteric ligand were removed. The optimization of protein was carried out by using Impref and minimization of energy was carried out using default constraints of 0.30 Å of RMSD and OPLS_2005 force field [20].

Receptor grid generation:

A 3D grid representing binding site of enzymes was generated around the co-crystallized ligands viz. FAD. The inhibitors of MurB and FAD share same binding site, therefore, FAD is regarded as co-crystallized ligand [9,11,21], using receptor grid generation panel of Glide module of Maestro software.

Validation of the docking protocol:

The validation of the docking protocol was done by docking of extracted co-crystallized ligand. The co-crystallized ligand of the PDB IDs 1HSK was extracted from the protein and docked into the prepared grid representing the binding site. The pose of the docked ligand and the co-crystallized ligands were superimposed and their RMSD was calculated [7].

Structure-Based Virtual Screening:

The virtual screening workflow panel of Maestro *v*11.2 software was used to carry out structure-based virtual screening (figure 1). In the panel, the downloaded .sdf file of zinc database comprising of 1000, 000,000+ molecules was added, its ligands were subjected to pharmacokinetic evaluation using QikProp and were filtered through and Lipinski filter. Thereafter, the ligands of the database were prepared at pH 7.0±2.0 using Epik and high energy ionization/ tautomer states were removed. Then, in the receptor tab prepared and validated grid of enzyme MurB (PDB ID: 1HSK) was added. Thereafter, docking was performed by HTVS, SP, and XP modes. The compounds to be kept after each docking method was specified as: 50% after HTVS, 40% after SP, and 30% after XP. The resultant hits were post processed by Prime-MM/GBSA to calculate the binding free energies of the ligand-receptor complexes. The interactions of selected hits with active site amino acids were visualized by using XP-Visualization.

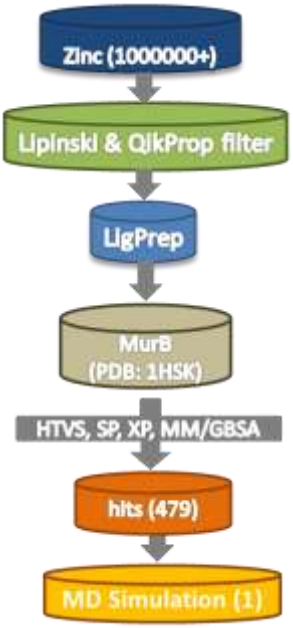

Figure 1: Flowchart of the research protocol.

Selection of Hits

The virtual screening protocol leads to identification of 479 hits. The hits that had XP GScore of less than -8.0 were screened for their pharmacokinetics.

QikProp descriptors viz. #stars, #rtvFG, CNS, Qplog HERG, QPP Caco, Qplog BB, QPP MDCK, #metab, human oral absorption, rule of five and rule of three were taken into consideration. #stars predict drug likeness, #rtvFG predict the presence of reactive functional group, presence of these groups can lead to false positives in assays or toxicity problems, QplogHERG predicts IC_{50} value for blockage of HERG K+ channels (present in heart), QPP Caco predicts apparent Caco-2 cell (model for the gut-blood barrier) permeability, CNS predicts central nervous system activity on a –2 (inactive) to +2 (active) scale, Qplog BB predicts brain/blood partition coefficient, QPP MDCK predicts MDCK cell (mimic for the blood brain barrier) permeability, #metab predicts number of likely metabolic reactions, human oral absorption predicts qualitative human oral absorption: 1, 2, or 3 for low, medium, or high, rule of five determines number of violations of Lipinski's rule of five, rule of three determines number of violations of Jorgensen's rule of three. The ligands that cross blood brain barrier may treat meningitis and brain abscesses, cases of which have also spiked recently.

The molecules that had values within the allowed ranges were selected. Thereafter, on the basis of MM/GBSA score, ligand pose, ligand-protein interactions molecule ZINC 34230491 was chosen for MD Simulation.

MD Simulations

The Desmond tool of Maestro software was used to pursue the molecular dynamics of the ligand-protein complex [22]. The selected molecule, viz., ZINC 34230491, was submitted for MD simulation. The simulation calculation was performed in three major steps, i.e., system builder, energy minimization, and molecular dynamics. A solvated system was generated by choosing SPC as the model solvent and POPC as the orthorhombic membrane. The buffer was specified for box size computation at a distance of 10.0. The physiological state of the simulation box was attained by neutralizing the charge and adjusting the salt content to 0.15 M for Na^+ and Cl^- ions. The volume of the simulation box is minimized by aligning the principal axes of the solute along the box vectors or the diagonal. The solute in the solvated system is composed of protein, protein complexes, protein-ligand complexes, protein encased in a bilayer membrane, etc. The energy of the ligand-protein complex was minimized by executing a 100 ps low-temperature (10 K) Brownian motion MD simulation (NVT ensemble) in order to eliminate

steric conflicts in the complex. The pre-processed ligand protein complex was loaded from the MD workspace and the NPT ensemble temperature and pressure were set to 300.0 K and 1.01325 bar, respectively. After model system relaxation, 100ns simulations were run and a trajectory was recorded at 4.8ps for the ligand-protein complex [23]. During the 100ns simulation, energy, ligand-protein RMSD, RMSF, protein-ligand interactions, and ligand characteristics were explored to determine the conformational behavior and stability of the complex.

Results & Discussion

Docking protocol validation through docking of co-crystallized ligand

The validation of the docking procedure was done by docking of extracted co-crystallized ligand FAD. The docking scores and the calculated RMSD values between the superimposed pose of docked ligand and extracted co-crystallized ligand are provided in figure 2. The protein–ligand interactions were also similar to those reported in the literature.

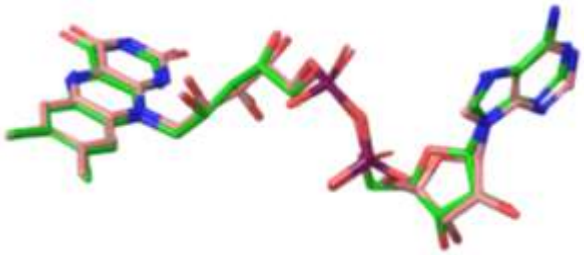

Figure 2: Superimposed image of Co-crystalized extracted ligand FAD (pink) and docked ligand (green), the RMSD between the two was found 0.1

Docking study

The docking images of top two selected compounds viz. ZINC 34230491 and ZINC 3872177 are provided in figures 3 and 4 respectively. Both the molecules bound well with the active site of the enzyme. The pose of the molecule ZINC 34230491 versus the pose of the molecule ZINC 3872177 (figure 4d) revealed that the former molecule fitted better in the enzyme cavity. Therefore, it was selected for pursuing further molecular dynamics study.

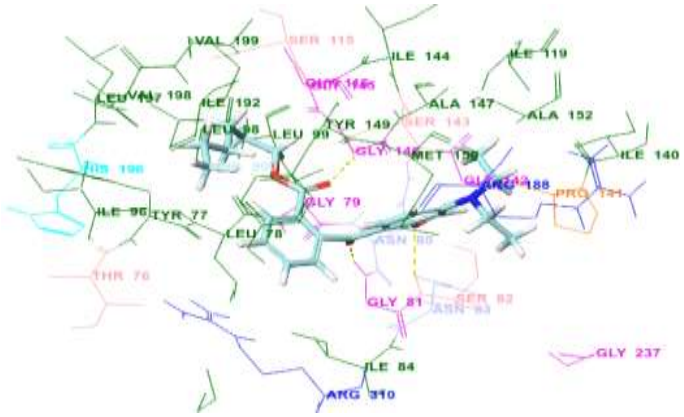

(a)

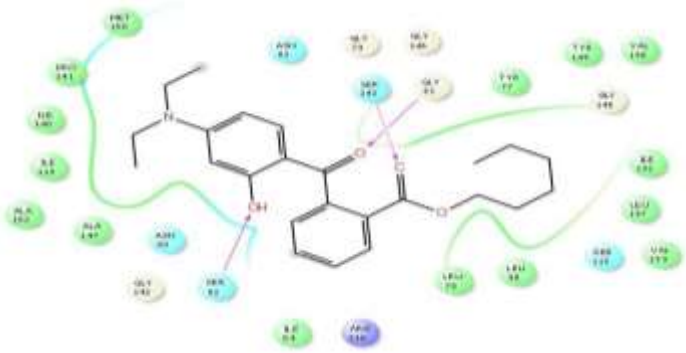

(b)

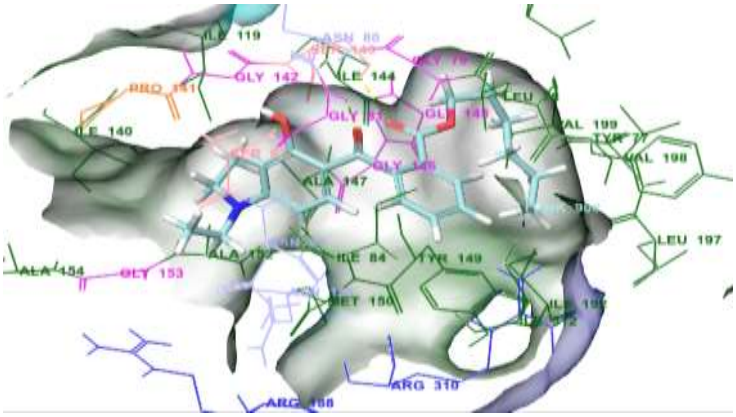

(c)

Figure 3: Docking image of selected compound ZINC 34230491 with 1HSK PDB ID of MurB protein. (a) Binding site residues interacting with selected ligand (b) 2D ligand interaction diagram (c) ligand interaction with protein within surface.

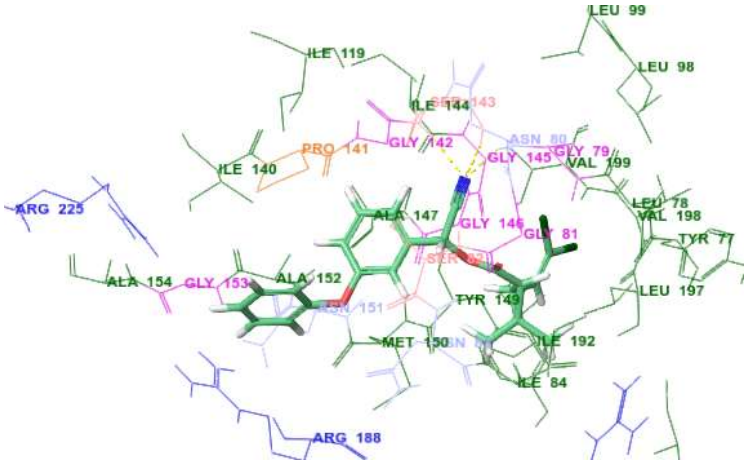
LEU 99
ILE 119
LEU 98
ILE 144
GLY 142
PRO 141
GLY 145
VAL 199
ILE 140
ARG 225
ALA 147
GLY 146
LEU 78
VAL 198
GLY 81
TYR 77
ALA 154
GLY 153
ALA 152
TYR 149
LEU 197
MET 130
ILE 192
ILE 84
ARG 188

(a)

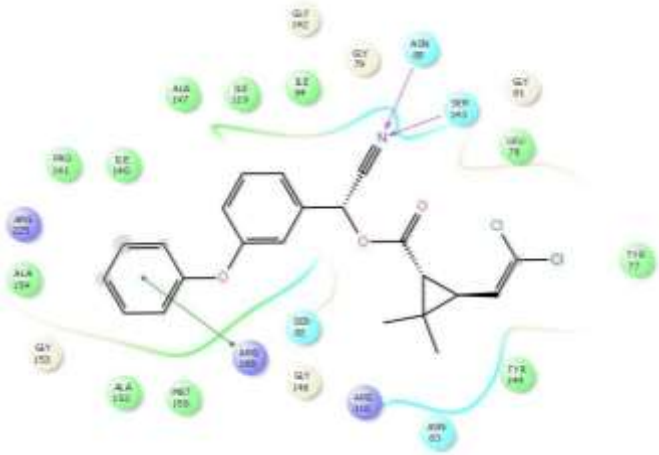

(b)

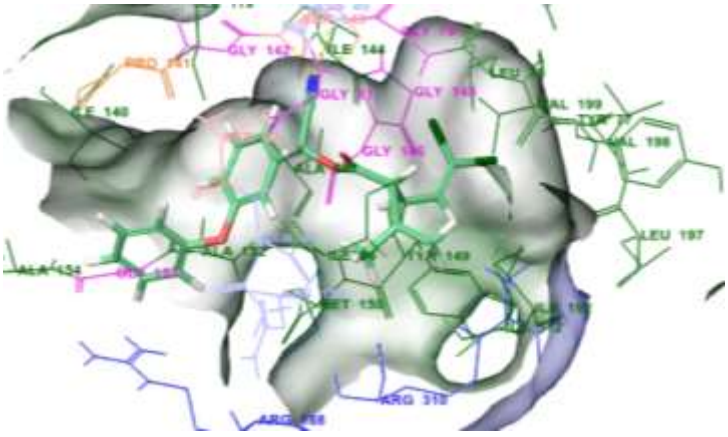

(c)

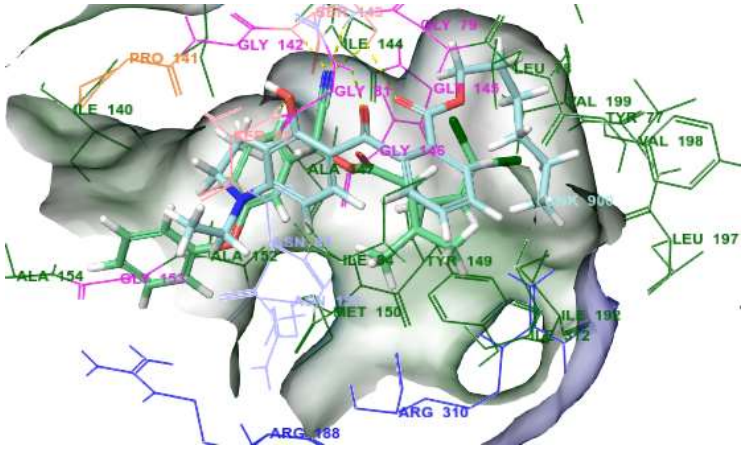

(d)

Figure 4: Docking image of compound ZINC 3872177 with 1HSK PDB ID of MurB protein. (a) Binding site residues interacting with selected ligand (b) 2D ligand interaction diagram (c) ligand interaction with protein within enzyme surface (d) superimposition of ZINC 34230491 (turquoise) with ZINC 3872177 (green) in enzyme pocket.

Table 1: Docking score (XP GScore), binding free energy estimation (MM/GBSA) of selected ligands of Zinc database against 1HSK PDB ID of MurB.

S. No.	Zinc ID	XP GScore	MMGBSA dG Bind
1	ZINC000034230491	-9.34	-106.91
2	ZINC000003872177	-9.23	-103.36
3	ZINC000000537804	-8.38	-100.52
4	ZINC000100037087	-9.38	-99.56
5	ZINC000000537802	-8.78	-97.99
6	ZINC000095617668	-8.78	-95.20
7	ZINC000095617669	-8.59	-94.26
8	ZINC000034303655	-8.50	-93.40
9	ZINC000005514233	-10.31	-92.09
10	ZINC000002015997	-8.12	-90.65
11	ZINC000095617667	-8.46	-88.59
12	ZINC000261494589	-8.46	-88.59
13	ZINC000021999791	-10.23	-85.82
14	ZINC000001704227	-11.35	-76.90
15	ZINC000001704226	-10.91	-71.88
16	ZINC000038929225	-10.21	-69.24
17	ZINC000001844627	-10.46	-58.79
18	ZINC000095618741	-11.09	-57.50
19	ZINC000006116336	-10.22	-47.62
20	ZINC000006116536	-10.24	-45.28

Table 2: ADME (QikProp) results of selected ligands of Zinc database against 1HSK PDB ID of MurB

S. No.	Zinc ID	#stars	#rtvFG	Qplog HERG	Human Oral Absorption	CNS	QPlogBB	QPPCaco	QPPMDCK	#metab	Rule of Five	Rule of Three
1	ZINC000034230491	0	1	-4.81	3	-2	-1.12	1000.89	495.18	2	0	0
2	ZINC000003872177	0	2	-4.23	3	0	-0.49	963.06	1543.16	2	0	0
3	ZINC000000537804	0	1	-4.86	2	-2	-2.51	48.49	27.48	2	0	1
4	ZINC000100037087	0	0	-4.35	3	-2	-1.20	162.34	658.42	3	0	0
5	ZINC000000537802	0	0	-4.79	2	-2	-2.48	52.16	27.79	2	0	1
6	ZINC000095617668	0	1	-3.77	3	-2	-1.46	141.57	90.02	2	0	0
7	ZINC000095617669	1	1	-4.15	3	-2	-1.62	102.44	76.15	2	0	0
8	ZINC000034303655	0	0	-3.07	3	-2	-1.36	159.34	96.08	5	0	0
9	ZINC000005514233	0	0	-4.94	3	-2	-1.66	219.48	96.04	3	0	0
10	ZINC000002015997	1	1	-3.75	3	0	-0.40	1515.89	2005.50	3	0	0
11	ZINC000095617667	0	1	-3.65	3	-2	-1.39	164.42	98.29	2	0	0
12	ZINC000261494589	0	1	-3.72	3	-2	-1.47	136.58	85.05	2	0	0
13	ZINC000021999791	0	1	-4.71	3	1	0.12	376.15	566.66	5	0	0
14	ZINC000001704227	0	1	-4.73	2	-1	-0.82	92.22	41.62	5	0	0
15	ZINC000001704226	0	1	-4.53	2	0	-0.58	160.02	75.52	5	0	0
16	ZINC000038929225	1	0	-3.19	3	-1	-0.99	155.62	555.17	3	0	0
17	ZINC000001844627	0	2	-4.89	3	0	-0.38	897.12	1274.21	3	0	0
18	ZINC000095618741	1	2	-4.08	3	-2	-1.26	69.66	27.78	2	0	0
19	ZINC000006116336	0	0	-4.49	3	-2	-1.35	90.02	36.65	3	0	0
20	ZINC000006116536	0	0	-4.55	3	-2	-1.34	94.26	38.52	3	0	0

MD Simulation

MD Simulation of 100ns of compound ZINC 34230491 was carried out against enzyme 1HSK PDB ID. The protein RMSD (x-axis) (figure 5a) changes are within the acceptable range (1-3 Å). The simulation converged (1.8 Å) at the end. This means the system got equilibrated, and the simulation was long enough for rigorous analysis. The bar graph (figure 5b) depicts the hydrophobic contacts established by compound ZINC 34230491 with residues Tyr149, Ile84, Leu98, Tyr77, Met150, Ala152, Ile192, Ile119, Ile40, Val198, and Val199. It indicates that Ser82, Asn83, Gly81, Gly142, and Gly79 were involved in the formation of hydrogen bonds with ZINC 34230491. The ligand formed hydrogen bonds with the amino acid residues Gly81, Gly142, Asn80, Ser82, Asn83, Pro141, Ser238, Gly237, and Arg310, by building water bridges. The predominant residues with which the ligand interacted were Ser82, Tyr149, Gly81, and Asn83. The ligand interacted with residues Asn83, Tyr149, Ser82, Asn80, and Gly81for more than 10% of the time during the simulation (figure 5c). The heat diagram represents the contacts between residues and the ligand on a timeline (figure 5d). The display exhibits the comprehensive count

of interactions established by the protein and the ligand throughout the trajectory. The residues Ser82, Gly81, Asn83, Tyr149, and Gly142 form multiple interactions with the ligand (indicated by a more pronounced orange coloration).

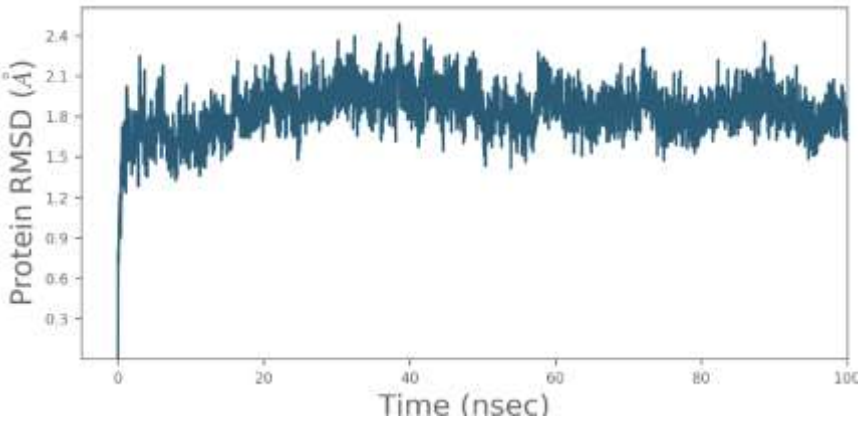

(a)

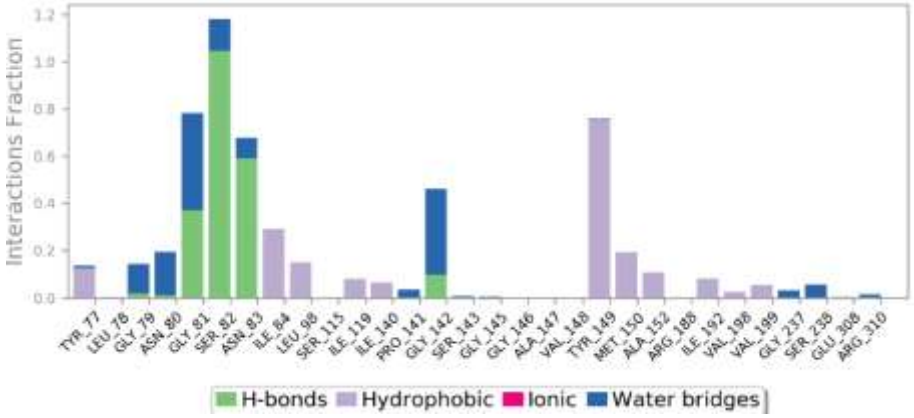

(b)

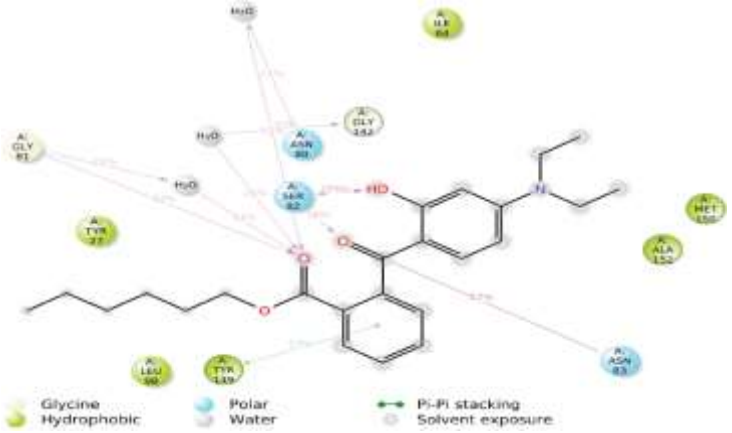

(c)

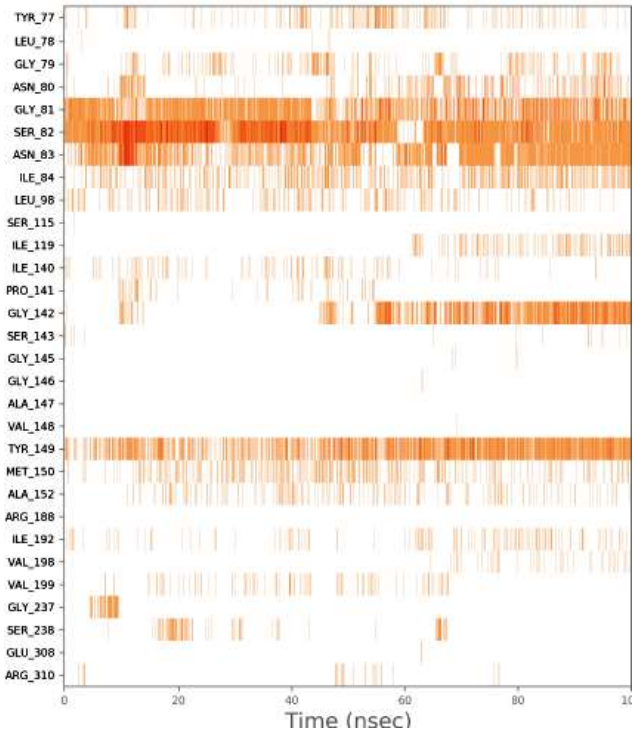

(d)

Figure 5: Results of MD simulation of ZINC 34230491 with 1HSK PDB ID. (a) Protein-Ligand RMSD of protein with ligand for 100 ns. (b) Protein-Ligand Contacts of protein with ligand (c) Ligand-Protein Contacts of ligand with protein. (d) Protein-Ligand Contacts (cont.) of protein with ligand.

Conclusion

Hit against 1HSK PDB ID of MurB enzyme for *S. aureus* pathogen were identified using structure-based virtual screening, ADME analysis, MM/GBSA, and MD Simulation studies. The identified hit ZINC 34230491 had no ADME property outside the prescribed range; it fitted the binding site of the enzyme well, and was found stable in MD simulation studies. This compound could be tested for anti-bacterial activity and further used as a lead to discover potential antimicrobial drugs against *S. aureus* pathogen.

Statements and Declarations

The authors declare that they have no known competing financial interests or personal relationships that could have appeared to influence the work reported in this paper.

References

[1]. Y. Guo, G. Song, M. Sun, J. Wang, Y. Wang, Front. Cell. Infect. Microbiol. 2020, 10.
[2]. X. Zheng, T. Zheng, Y. Liao, L. Luo, Molecules 2021, 26, DOI 10.3390/molecules26216426.
[3]. G. Y. C. Cheung, J. S. Bae, M. Otto, Virulence 2021, 12, 547–569.
[4]. R. M. Klevens, M. A. Morrison, J. Nadle, S. Petit, K. Gershman, S. Ray, L. H. Harrison, R. Lynfield, G. Dumyati, J. M. Townes, et al., JAMA 2007, 298, 1763–1771.
[5]. S. J. van Hal, S. O. Jensen, V. L. Vaska, B. A. Espedido, D. L. Paterson, I. B. Gosbell, Clin. Microbiol. Rev. 2012, 25, 362–386.
[6]. A. Koutsoukas, B. Simms, J. Kirchmair, P. J. Bond, A. V. Whitmore, S. Zimmer, M. P. Young, J. L. Jenkins, M. Glick, R. C. Glen, et al., J. Proteomics 2011, 74, 2554–2574.
[7]. A. Shrivastava, S. Srivastava, R. Malik, M. M. Alam, M. Shaqiquzamman, M. Akhter, J. Biomol. Struct. Dyn. 2020, 38, DOI 10.1080/07391102.2019.1602078.
[8]. T. E. Benson, M. S. Harris, G. H. Choi, J. I. Cialdella, J. T. Herberg, Martin Joseph P., E. T. Baldwin, Biochemistry 2001, 40, 2340–2350.
[9]. A. M. AboulMagd, N. M. Eid, A. H. Korany, A. O. El-Gendy, H. M. Abdel-Rahman, Egypt. J. Chem. 2020, 63, 4355–4367.
[10]. T. Shi, Q. Ma, X. Liu, Y. Hao, Y. Li, Q. Xu, X. Xie, N. Chen, Bioengineered 2019, 10, 548–560.
[11]. Y. Yang, A. Severin, R. Chopra, G. Krishnamurthy, G. Singh, W. Hu, D. Keeney, K. Svenson, P. J. Petersen, P. Labthavikul, et al., Antimicrob. Agents Chemother. 2006, 50, 556–564.
[12]. T. D. Bugg, C. T. Walsh, Nat. Prod. Rep. 1992, 9, 199–215.
[13]. J. S. Anderson, M. Matsuhashi, M. A. Haskin, J. L. Strominger, J. Biol. Chem. 1967, 242, 3180–3190.
[14]. D. Mengin-Lecreulx, B. Flouret, J. van Heijenoort, J. Bacteriol. 1982, 151, 1109–1117.
[15]. T. E. Benson, J. L. Marquardt, A. C. Marquardt, F. A. Etzkorn, C. T. Walsh, Biochemistry 1993, 32, 2024–2030.
[16]. T. E. Benson, C. T. Walsh, V. Massey, Biochemistry 1997, 36, 796–805.
[17]. D. R. Sylvester, E. Alvarez, A. Patel, K. Ratnam, H. Kallender, N. G. Wallis, Biochem. J. 2001, 355, 431–435.
[18]. A. H. Katz, C. E. Caufield, Curr. Pharm. Des. 2003, 9, 857–866.
[19]. C. D. Haffner, C. J. Diaz, A. B. Miller, R. A. Reid, K. P. Madauss, A. Hassell, M. H. Hanlon, D. J. T. Porter, J. D. Becherer, L. H. Carter, Bioorganic Med. Chem. Lett. 2008, 18, 4360–4363.
[20]. W. L. Jorgensen, J. Tirado-Rives, J. Am. Chem. Soc. 1988, DOI 10.1021/ja00214a001.
[21]. A. Maitra, T. Munshi, J. Healy, L. T. Martin, W. Vollmer, N. H. Keep, S. Bhakta, FEMS Microbiol. Rev. 2019, 43, 548–575.

[22]. K. J. Bowers, D. E. Chow, H. Xu, R. O. Dror, M. P. Eastwood, B. A. Gregersen, J. L. Klepeis, I. Kolossvary, M. A. Moraes, F. D. Sacerdoti, et al., in SC ’06 Proc. 2006 ACM/IEEE Conf. Supercomput., 2006, p. 43.

[23]. D. Shivakumar, J. Williams, Y. Wu, W. Damm, J. Shelley, W. Sherman, J. Chem. Theory Comput. 2010, 6, 1509–1519.